Spring 2019

An Upper Extremity Exoskeleton Utilizing a Modified Double Parallelogram Linkage Mechanism with Proximally Located Actuators

Connor Bouffard

University of Maine

Recommended Citation

AN UPPER EXTREMITY EXOSKELETON UTILIZING A MODIFIED DOUBLE

PARALLELOGRAM LINKAGE MECHANISM WITH PROXIMALLY LOCATED

ACTUATORS

by

Connor M. E. Bouffard

A Thesis Submitted in Partial Fulfillment
of the Requirements for a Degree with Honors
(Mechanical Engineering)

The Honors College

University of Maine

May 2019

Advisory Committee:
    Babak Hejrati, Assistant Professor of Mechanical Engineering, Advisor
    François Amar, Dean of the Honors College & Professor of Chemistry
    Vincent Caccese, Professor of Mechanical Engineering
    Andrew Goupee, Assistant Professor of Mechanical Engineering
    Mohsen Shahinpoor, Professor of Mechanical Engineering

ABSTRACT

The shoulder joint is an extremely complex joint, with a wide range of motion (ROM), which makes designing an upper extremity exoskeleton a complicated task. This thesis presents a 3-degree-of-freedom (DOF) exoskeleton with a modified double parallelogram mechanism (DPM) that fits any wearer independent of their biological frame. The DPM is remarkably useful in wearable robotics. The mechanism creates a remote center of rotation about the shoulder joint while remaining unobtrusive and not colliding with the wearer's body. Its fixed link lengths, however, requires it to be specially fitted to each individual user. This is inconvenient for most exoskeletons that utilize a DPM, since wearers often vary in body shape, size, and build. By connecting the two parallelograms with a mediating link and implementing a sliding-pin joint, the proposed modified DPM allows for a much larger ROM than the original design of the mechanism. This allows it to fit onto almost any anthropometric frame. The exoskeleton provides active assistance during flexion/extension while allowing free abduction/adduction and internal/external rotations. The experimental results demonstrate the proposed design's ability to provide assistance during a wide range of shoulder motions.

ACKNOWLEDGEMENTS

First and foremost I would like to thank my parents, Brian and Kenda Bouffard, for their unwavering love and support. Through the sixteen years that I have been in school, they have done nothing but foster an environment for my development and success. I could not be more grateful for them. On top of that, I would like to thank my group of friends for making my college career exciting and memorable.

I would like to thank Michael Jones for his help and support throughout the thesis process. He and I have been working on the same project for approximately one year, and he has been absolutely crucial to the design of the presented device. Lastly, I would like to thank my advisor, Babak Hejrati, and my committee members for their support and technical advice. Their availability to answer any questions I had during the design process was extremely helpful, and lead to a functioning prototype. Without everyone mentioned, I would not be where I am today.

TABLE OF CONTENTS

LIST OF TABLES

INTRODUCTION

Robotic exoskeletons are becoming increasingly popular in neuromuscular

rehabilitation and daily task assistance methods. When designing exoskeletons there are

many parameters that must be considered. For instances, the design must be ergonomic

and comfortable for the wearer. An ergonomic design typically includes multiple passive

degrees of freedom (DOF) to prevent the exoskeleton from restricting any movements of

the wearer. In addition, the design should not collide with the wearer during assistive

movements or be obtrusive in any way. Accounting for these parameters is especially

difficult when designing an exoskeleton for the shoulder. The shoulder joint has multiple

movement patterns across multiple movement planes and makes creating an exoskeleton

challenging.

The design of Hsieh et al. [1] addresses the complexity of the shoulder joint by

utilizing two linear actuators, a 4-revolute (4R) spherical mechanism, and a 5-revolute

(5R) spherical mechanism. The design has 2 powered DOFs, and 4 passive DOFs. The

multiple passive DOFs prevent any potential joint misalignments while the exoskeleton is

in use. This improved ergonomics, however, also increased the design's complexity and

bulkiness. There are multiple moving parts that add to the potential of design failure, and

the presence of the 5R mechanism on top of the shoulder may be obtrusive to some users.

In addition, flexion/extension is achieved by actuating internal/external and

abduction/adduction rotations simultaneously. Accomplishing flexion/extension, in the

sagittal plane, may overextend the mechanism and result in stiffness issues.

Our design team desires an exoskeleton that is simple, low profile, and unobtrusive while directly powering flexion/extension. All these qualities should be accomplished by the exoskeleton while maintaining ergonomics and avoiding any joint misalignments.

An exoskeleton that accomplishes some of these qualities is the design of [2]. By utilizing a double parallelogram mechanism (DPM) the exoskeleton is less complicated and obtrusive than the exoskeleton by Hsieh et al. [1], while maintaining comparable ergonomics. This design has passive internal/external rotation and active abduction/adduction and flexion/extension rotation. The DPM forms a remote center of rotation about the humeral head of the user's shoulder and will prevent any joint misalignment during internal/external rotation. This is assuming the design is fitted to the anthropomorphic frame of the wearer.

When determining the link lengths of the DPM, Christensen et al. [2] simplified the shoulder to a sphere whose diameter was determined using data gathered by Peebles et al. [3]. The ergonomics of a DPM, however, is highly dependent upon how well it is sized to the individual body of the wearer. Since wearers have varying body sizes, a standardized exoskeleton will not fit everyone ideally.

This thesis presents an exoskeleton utilizing a modified DPM with a much larger range of motion (ROM) than the original design. The increased ROM of the modified DPM allows the presented exoskeleton to fit onto a large range of users and negates the need for a specially fitted exoskeleton. This design is based on the design proposed by Christensen et al. [2], where the original DPM is used. The proposed exoskeleton has 3 DOFs with powered flexion/extension and passive abduction/adduction and

intern/external rotations. In this paper, the proof of concept of the design is presented.

Also, a forward kinematic analysis is presented to demonstrate the ROM of the design.

Finally, a prototype is fabricated and tested.

LITERATURE REVIEW

Robotic exoskeletons are becoming increasingly popular in neuromuscular rehabilitation methods and daily task assistance; however, many designs are fixed to a desk, wall, or another structure that prevents the free movement of users [4 – 6]. These stationary devices can be improved remarkably by increasing their range of mobility. Redesigning stationary devices into backpack mountable models is a promising avenue for more user-friendly exoskeletons. Although a mobile, wearable exoskeleton design seems like a simple improvement to a stationary rehabilitation robot, it comes with its own plethora of complications. Most notably, one must consider the exoskeleton's weight and weight placement on the wearer. In addition, factors common to both mobile and stationary designs, including torque transmission and ergonomics must be addressed. These parameters are often determined by the exoskeleton's intended application. For example, if an exoskeleton is intended to be used for an industrial application it will be required to generate a substantial amount of torque, be extremely robust, and fairly comfortable to wear. As such, designers must employ relatively large actuators, rigid links, and multiple passive DOFs to fulfill the requirements simultaneously. If the exoskeleton is intended to be used by civilians for daily living tasks, however, torque generation and robustness would become less important while ergonomics would take precedence. In both scenarios all three parameters are important, but the exoskeleton's application determines how important each parameter is.

Lightweight, Low Torque Versus Heavy, High Torque

As one might imagine, high torque generating exoskeletons are typically heavier than their low-torque counterparts. This is due to the size of the actuators required to generate large amounts of torque. Large actuators are not only heavier than small actuators but also require a more robust frame to be mounted on. One can create a more robust frame by changing the material it is made of or by changing its physical size. The increase in the actuator size and a proportional increase in the frame robustness can have a substantial impact on the weight of the exoskeleton.

When comparing wearable exoskeleton designs, it should be noted that the difference between what is deemed as light and heavy, while subjective, is on the scale of only a few kilograms. For an exoskeleton that is intended to be used for rehabilitation and daily task assistance, the weight should not exceed 10% of the wearer's body weight – a conventional standard for hiking backpacks [7]. Assuming a 75 kg person, the exoskeletons should not weight more than 7.5 kg. Similarly, what is deemed as a low torque generating exoskeleton is subjective and will be classified here as anything below 10 N.m.

Making an accurate comparison of current designs is a challenging task. Different designs are at varying points in the prototyping process; therefore, it is difficult to gather accurate weight measurements that can be compared. In addition, there isn't a standard way authors record torque generation, so comparing these values may be challenging as well. In some cases, the weight or torque values might not even be reported. None-the-less, we can examine exoskeleton designs and draw conclusions to determine the relationship between these two parameters: weight and torque generation.

Figure 1 (a), the design of Liu et. al. [8] can provide powered assistance up to 30% of a human's mass during flexion/extension. The design has two powered and two passive DOFs. Flat Maxon 75 watt brushless DC motors (140 grams) are employed to actuate flexion/extension of both the shoulder and elbow joints, while medial supination/pronation of the shoulder and abduction/adduction of the forearm are passive. The motors for each active joint are connected to harmonic drives via a pulley system which results in a 300:1 gear ratio that ultimately rotates the wearer's arm at 90 degrees per second. The design utilizes aluminum for structural parts, Carbon Fiber Reinforced Plastic for nonstructural parts, and acrylic resign for complex shaped parts of the frame work. By virtue of the lightweight frame materials, relatively small motors and harmonic drives, and the low torque requirement this design only weights 5.1 kg – well under the targeted weight.

The design by Christensen et al. [2], Figure 1 (d), provides power assistance up to 50% a human's mass. The design has 3 active and 1 passive DOFs, powering shoulder abduction/adduction and flexion/extension and elbow flexion/extension. Three Maxon EC 60 brushless DC motors (2400 grams) are used to actuate the active DOFs. The motors are directly connected to harmonic drives at each joint's axis of rotation. While the exoskeleton's total weight is not reported, we can calculate a projected minimum weight from the mass of the motors and other hardware. Accounting for the 6 actuators and 2 double parallelogram linkages (200 grams) the minimum mass of the exoskeleton would be 15.2 kg. This value isn't accounting for the mass of the backpack nor the mass of the rigid links and cuffs that attach to the wearer's torso and arms. So while the exoskeleton by Christensen et al. [2] can generate substantially more torque than the

exoskeleton by Liu et al. [8], it is also at least 3 times heavier. Neither exoskeleton is better or worse than the other: they were simply designed and sized for their respective intended applications.

From the designs in Figure 1 (a) and (d) we can surmise lighter weight exoskeletons generate lower torques than heavier exoskeletons. This trend can also be seen in lightweight designs shown in Figure 1 (b) and (c) and heavy designs Figure 1 (e), and (f).

Figures 1 (b) and (c) utilize spring-based gravity balancing mechanisms to shift the bulk of the exoskeleton's weight to the wearer's hips. This weight can then be passed to the lower extremities exoskeleton and transferred directly to the ground. When wearing Figure 1 (b), the design of Park [6], the user only experiences 2.72 kg per arm for a total weight of 5.44 kg. This exoskeleton has powered shoulder flexion/extension and abduction/adduction and is capable of generating 15-20 N-m of torque. Figure 1 (c), the design by Sui et al. [10], provides 4 active and 1 passive DOFs and weights 8.4 kg for both arms. Unfortunately, output torque values and motor sizes were not reported.

Figures 1 (e) and (f) are examples of high torque generating designs from Carignan et al. [11] and Ebrahimi et al. [12] respectively. Figure 1 (e) weighs 24 kg for both arms, has 5 active DOFs, and can generate up to 30 N-m of torque for shoulder flexion/extension. Figure 1 (f) has 3 active and 9 passive DOFs and can generate up to 40 N-m of torque for shoulder flexion/extension and up to 24 N-m of torque for elbow flexion/extension. The exoskeleton's mass was not reported.
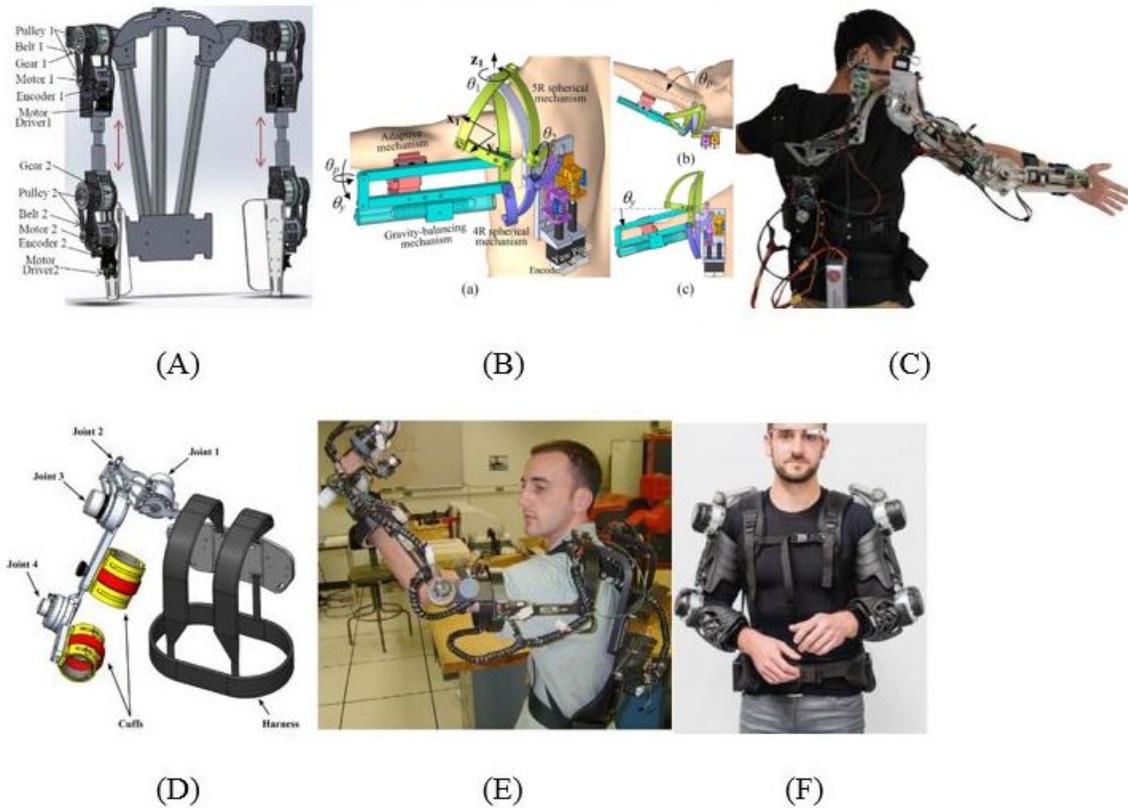
Figure 1 Examples of light weight, low torque and heavy, high torque exoskeletons (A) Liu et. al. [8] (B) Hsieh et. al. [1] (C) Sui et. al [10] (D) Christensen et. al. [2] (E) Carignan et. al. [11] (5) Ebrahimi et. al. [12]

<u>Rigid Links Versus Cable Driven</u>

In both types of exoskeletons, the ones that employ rigid links and are cable driven, DC motors are typically used to actuate the exoskeletons. There are some designs that utilize pneumatic actuators [13]; however, these are often too heavy to be carried on a user's back and as such will not be discussed in this paper.

It has been known that anatomical joints are hardly ever perfectly revolute [14]. With this being said, an exoskeleton with a single axis joint leads to misalignment between the wearer and the exoskeleton. This misalignment can cause discomfort for the wearer or even pain and injury. Implementing multiple passive DOFs into joint designs is

a common method used to mitigate misalignment between anatomical and artificial axes of rotation.

The design of Liu et al. [8] shown in Figure 1 (A) and Figure 2 (B) has a shoulder joint with 3 DOFs, one active and two passive. In Figure 2 (B) the first and third DOFs are passive and allow for scapular movement during shoulder raising. This compensation allows the active DOF to rotate ergonomically despite a moving axis of rotation.

The design of Christensen et al. [2] shown if Figure 1 (D), and again in Figure 2 (A), utilizes a double parallelogram linkage (DPL) to achieve 3 DOFs at the shoulder. The exoskeleton powers shoulder abduction/adduction and flexion/extension resulting in two active and one passive DOFs. The DPL shown in Figure 2 (A), creates a remote center that moves with the shoulder to reduce joint misalignment. Having only 1 passive DOF; however, means that an adaptive control algorithm will need to be implemented to actively sense when the shoulder joint is moving. In particular, the motor responsible for abduction/adduction will also need to account for scapula elevation and depression. Overall the exoskeleton is reported to have good mobility.

Hsieh et al. [1] replaced DC motors with linear stepper motors. This actuator change allowed them to use two slider-crank mechanisms and two spherical mechanisms to design a shoulder joint with 2 active and 4 passive DOFs. Figure 2 (C), shows the 5R and 4R spherical mechanisms used to power shoulder flexion/extension and abduction/adduction. By utilizing linear stepper motors with spherical mechanisms Hsieh et al. [1] was able to design a minimally invasive, compact, lightweight shoulder joint.

When using rigid links in an exoskeleton, each link's orientation angle can be easily tracked by placing an encoder at the joints. This makes control algorithms

9

relatively simple and allows for accurate control of the exoskeleton. On the other hand, joint misalignments while minimized are still prevalent due to the inflexible nature of the rigid links. In addition, rigid-link frames are often intrusive and not gentle for users to wear. A solution to completely get rid of joint misalignments and have a more ergonomic exoskeleton, is to use a cable driven system.

Such a system can be seen in Figure 2 (D), a design by Cappello et. al. [15]. This design places the actuating system on the wearer's back and runs cables across the shoulder joint. The cables use Bowden sheaths and have rigid cuff-like connections on the wearer to raise the arm. The absence of rigid links will completely mitigate joint misalignment since there isn't an artificial joint to be misaligned from. In addition, since there is no need for a large frame in this design, one can surmise that it is not only light weight but also comfortable to wear. These qualities make the exoskeleton extremely ergonomic. This style of design falls under the umbrella of soft robotics and is known for having a less intrusive interaction with wearers than conventional exoskeletons which use rigid links.

While soft robots excel in ergonomics, they lack in and control and movement accuracy. Designers of soft robotic exoskeletons must recognize the multitude of physical limitations that cable driven systems have: slacking, backlashing, slippage, and friction in Bowden sheaths. Dinh [16] attempted to mitigate slacking and backlashing by pre-tensioning the cables and using a nonlinear adaptive controller to actuate the system. Slippage between the wearer's arm and the exoskeleton was addressed by using tighter arm cuffs. Finally, friction was tackled by using PTFE lined Bowden sheaths. Even with

these mechanical and electrical solutions, joint movement inaccuracies are still a major

dilemma needing further attention.

Cable driven systems are lightweight and extremely ergonomic while being hard

to control. On the other hand, rigid link systems are easy to control but are typically

heavier and less ergonomic. When choosing between which type of exoskeleton to

employ, designers must assess their application's requirements and pick accordingly.
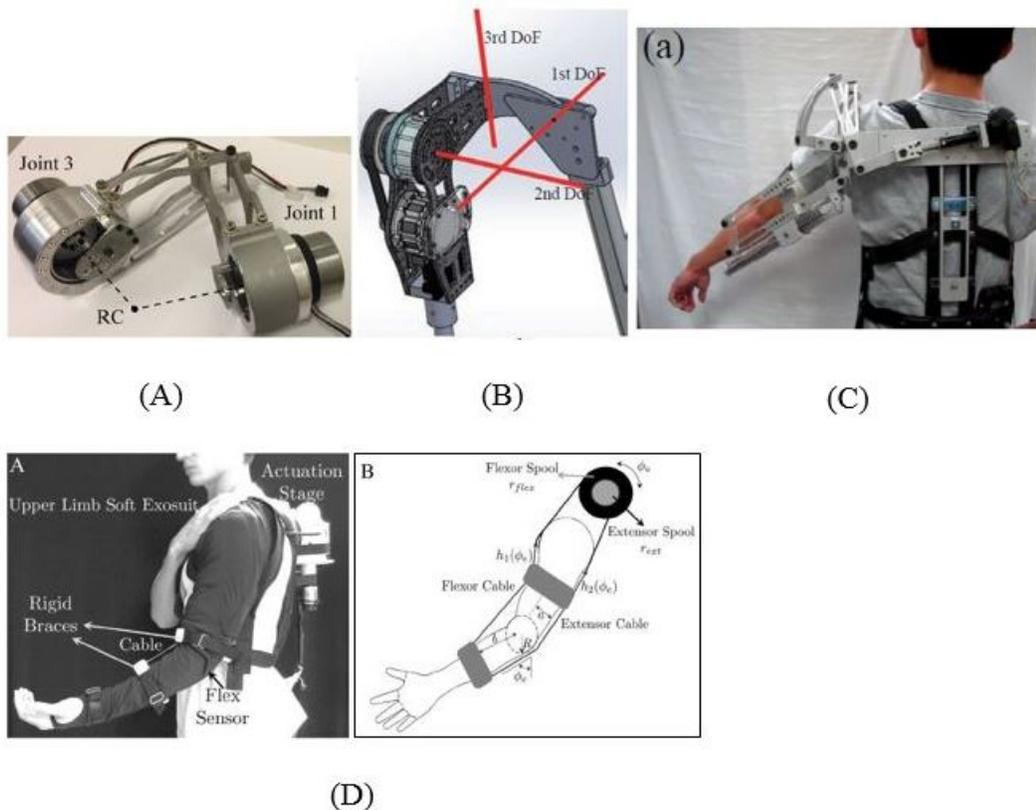
Figure 2 (A) Christensen et. al. [2] (B) Liu et. al. [8] (C) Hsieh et. at. [1] (D) Cappello et. al. [15].

Locally Versus Distally Mounted Actuators

When designing wearable exoskeletons, the location where weight is mounted on

the wearer is of the utmost importance. Placing a large amount of weight at the end of the

user's arm, for example, will create large moments about the shoulder joint. This will

require the motors actuating flexion/extension and abduction/adduction to work unnecessarily hard. Moving mass closer to the wearer's torso is a far more efficient and effective design strategy.

Placement of weight along the torso is also crucial. Typically, motors are mounted on the upper back while batteries reside just above the hips. Mounting motors on the upper back places them closer to the shoulders making it easy to transmit their power to and across such a complex joint. As previously discussed, Figures 1 (D) and (F) have motor placements on the upper back for abduction/adduction and the side of the shoulder for flexion/extension. While this design is simple it is not as efficient as it could be. Moving the actuators to the back as in Figure 2 (C) removes a large amount of weight from the arm, thereby reducing the moment induced on the shoulder joint. Cable driven systems, as in Figure 2 (D) are also very effective in actuator placement. A negligible amount of weight is placed on the wearer's arms, again inducing a minuscule moment.

A 2007 study conducted by Abe et al. [17] found that carrying weight on one's upper back is more energy efficient than carrying the same weight on the lower back. The study measured oxygen consumption as 14 men walked on a treadmill with 15% of their respective body weights placed on their upper and lower backs. In addition, a 2011 study conducted by Simpson et al [18] examined the effects of load placement on female hikers. In this study, 15 experienced female hikers traversed a 2 km simulated hiking trail carrying 30% of their body weights at a high, medium, and low position along on their backs. Electromyography (EMG), ground reaction force (GRF), and subjective preference data was collected. While there were slightly less discomforts reported for load placement on the lower back than upper, the majority of participants preferred a

higher load placement over medium or low. A higher load placement corresponded to a decrease in gastrocnemius EMG activation and an increase in GRF deceleration impact peak. Despite this data the authors admit that an ideal load placement location cannot be recommended and should be determined based of the individual's preference. This suggests an exoskeleton with the ability to move where the weight is located would be ideal.

Like most things, exoskeleton design is largely based on the desired functionality. An exoskeleton that is required to only supply 15 N.m of torque assistance during shoulder flexion/extension does not need to use extremely large actuators that will unnecessarily add mass to the design. Similarly, an exoskeleton that must generate 40 N.m of torque cannot use small actuators whose stall torque is well under this desired value. Designers must realize that every aspect of an exoskeleton has advantages as well as limitations, and this paper attempted to highlight a few of the most common.

PRELIMINARY DESIGNS

Design Iteration 1

The first exoskeleton was designed with simplicity in mind. This design has powered flexion/extension and passive abduction/adduction. A linear slider between the two mounting points was intended to allow for various sized wearers, however, this adjustability was only accounted for along the back of the wearer. One can deduce that, when the exoskeleton is worn like a backpack, the linear slider will allow for variation in the breadth of the back of the wearer. The thickness of the back of the wearer was neglected. In other words, adjustability perpendicular to the back is not included. It was determined that this lack of adjustability would not allow for internal/eternal rotation and would make the wearer feel restricted when worn.

Figure 3 Design iteration 1

Design Iteration 2

The second design iteration sacrificed simplicity for adjustability. Two scissor linkages allow for adjustability in both the breadth and thickness of the wearer's back. This design is worn in the identical fashion as design iteration 1, but for simplicity only the back plate was shown. The two scissor linkages can increase or decrease in length to fit onto various sized wearers, and the rotary joint between them can allow for internal/external rotation. Therefore, this design has powered flexion/extension and passive internal/external rotation and abduction/adduction rotations.

This design, however, was not prototyped for two reasons. First, this exoskeleton seemed to lack rigidity. In order for the exoskeleton to assist the movement of the wearer, it must be rigid enough to withstand the torque being transmitted. It was predicted this design could not withstand any significant amount of torque. The second reason concerns safety of the design during use. With multiple pitch points in the design, commercial use of this exoskeleton may not be the safest. For these reasons, this design was not furthered.
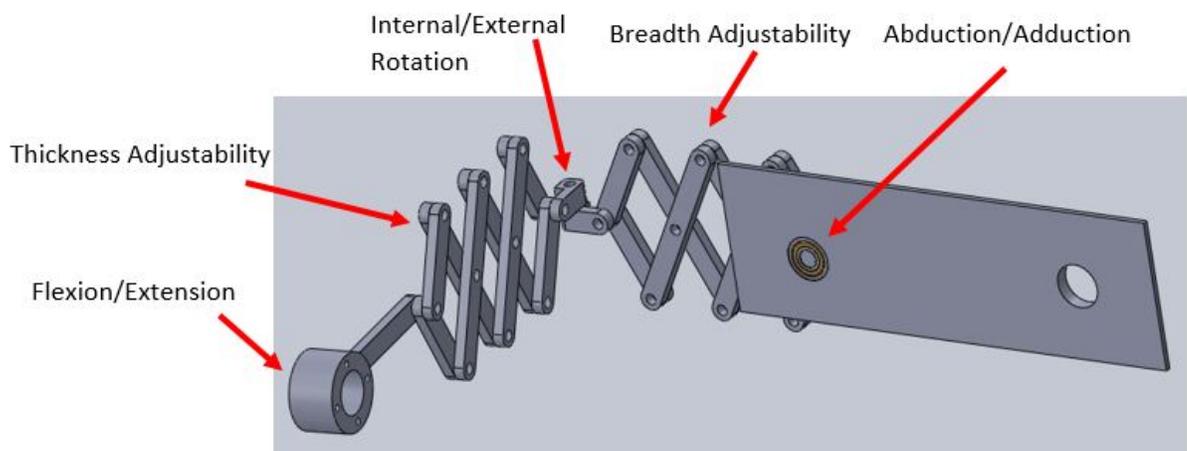
Figure 4 Design Iteration 2

Design Iteration 3

The third design iteration attempted to achieve internal/external rotation while remaining rigid and safe. A curved rail wrapped around the shoulder of the wearer, and the motor was mounted to the rail with a slider. This mechanism would allow for a fixed radius of rotation about the shoulder joint of the wearer, which allows for internal/external rotation. The motor would power flexion/extension, and a rotary bearing would allow for abduction/adduction.

Two problems were evident in this design. First, since the rail has a fixed, curved radius it is not adjustable and cannot fit onto to different wearers. Secondly, since the rail wraps around the shoulder of the wearer it would constantly be in front of the wearer. This is cumbersome and not ideal. A mechanism that extends during internal rotation and collapses during external rotation would be ideal. Such a mechanism is presented in this thesis and is the cumulating exoskeleton in the design iteration process.

Slider for Internal External/Rotation

Curved Rail

Abduction/Adduction

Flexion/Extension

Figure 5 Design Iteration 3

CONCEPTUAL DESIGN

The proposed exoskeleton utilizes a modified DPM with a proximally located actuator. The modified DPM allows for ergonomic and passive internal/external rotation. While the proximally located actuator provides flexion/extension assistance. The proximal location of the actuator was chosen for its simplicity. Placing the actuator directly on the joint mitigates the need for additional mechanisms that may be unnecessarily complex or cumbersome. The exoskeleton will be mounted on a backpack via a rotary bearing. This will allow for passive abduction/adduction.

Original DPM Design

The conventional DPM, shown inFigure 6**Error! Reference source not found.** Figure 6**Error! Reference source not found.**, is made of six links with seven axes of r otation. Links (1) and (2) are fixed to the wearer's back and arm respectively. Links (3) to (6) comprise the remaining sides of the two parallelograms. Two four-sided geometric shapes are formed with only six links because links (4) and (5) are both a short, and long, side of the parallelograms. This is, they are composed of both the labeled side, (4), and the adjacent side of the opposite parallelogram of the same color. What results is a sturdy mechanism that strictly rotates about a remote center (RC).
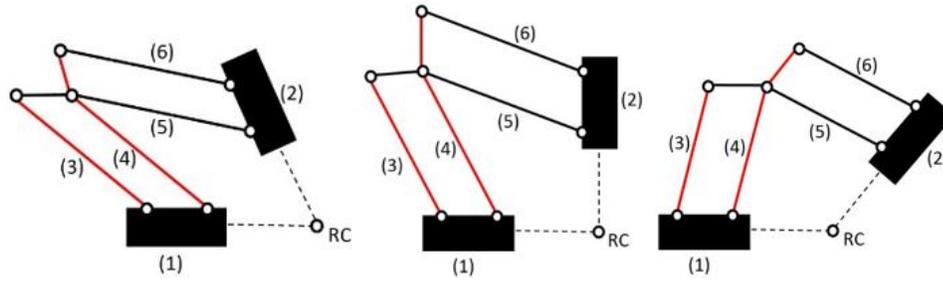
Figure 6 Original Design of Double Parallelogram Mechanism

The DPM rotates about the RC with a fixed radius. This radius of rotation can be adjusted to any desired value, however, this requires altering the lengths of links (3) to (6). Altering the link lengths will require an entirely new mechanism to be fabricated and installed on the exoskeleton. Since wearers vary in terms of their anthropomorphic measurements, a new exoskeleton will be needed for each wearer. This is extremely impractical. If the exoskeleton is not specially fitted to the wearer, joint misalignment will occur during internal/external rotation which could result in pain or even injury during use.

Modified DPM Design

The proposed, modified DPM includes seven links and seven axes of rotation, it is shown in Figure 7 below. Similar to the original design, links (1) and (2) are attached to the back and arm of the wearer respectively. The additional link, (7), is a mediating link that joins the two parallelograms in the mechanism. Links (3) to (5) all have the same length, and link (6) is a sliding-pin joint.

20
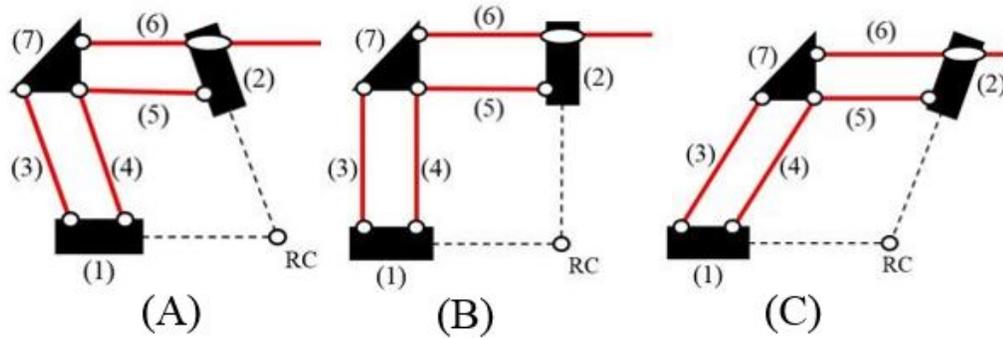
Figure 7 Modified design of Double Parallelogram Linkage

In use, link (1) will be mounted on the upper back of the wearer via a rotary bearing, and link (2) will house the actuator and be attached to the upper arm of the wearer. As the mechanism actuates, the orientation of link (2) changes to remain perpendicular to the arm of the wearer. This is possible due to the sliding-pin joint of link (6). It can be seen that as the mechanism actuates, the length of link (6) changes, and enables the mechanism to form a RC. This RC, however, does not have a fixed radius. By using link (7) as a mediating link between the two parallelograms, they are able to move independently of one another. That is parallelogram 1-3-7-4 can rotate without affecting parallelogram 2-5-7-6, and vice versa. Effectively, parallelogram 1-3-7-4 controls the placement of the end effector in the x-axis, while parallelogram 2-5-7-6 controls the placement in the y-axis. This is shown in Figure 8 and Figure 9 respectively.

21
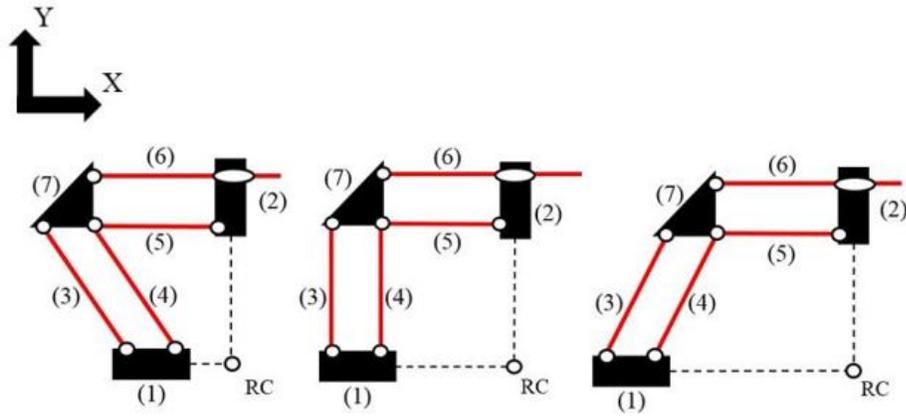
Figure 8 Rotation of Parallelogram 1-3-7-4
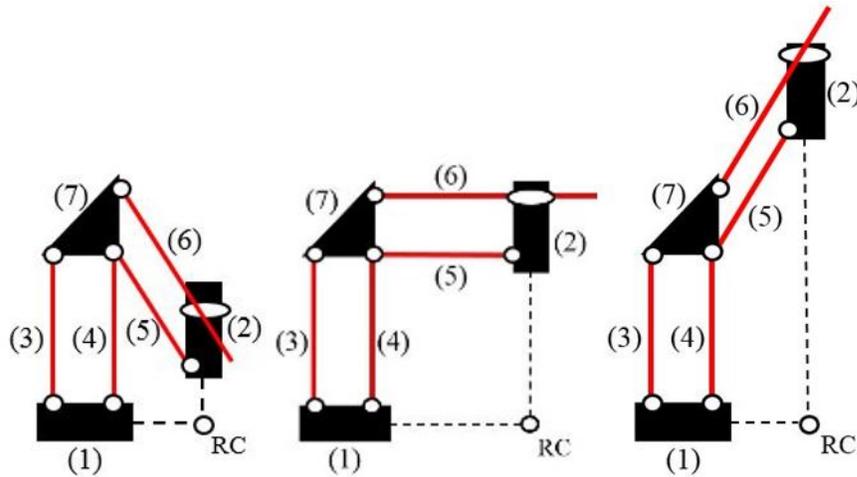
Figure 9 Rotation of Parallelogram 2-5-7-6

Forward Kinematic Analysis

Links (4) and (5) are pinned together through link (7), and effectively behave similar

to a two-degree-of-freedom, serial-link robot. In fact, links (4) and (5) are exactly a two-

degree-of-freedom, serial-link robot, and links (3) and (6) provide appropriate articulation

boundaries for the mechanism. These boundaries were directly measured from the 3D

printed prototype and are presented in Table 1 below. Figure 10 depicts the exoskeleton

configuration used to determine its DH parameters. This configuration is not the zero-angle position of the mechanism since the zero-angle position is unintuitive and impractical; rather, the presented configuration resembles how the exoskeleton would be worn. The axes of rotation are also shown in Figure 11 on the 3D printed prototype for clarification.
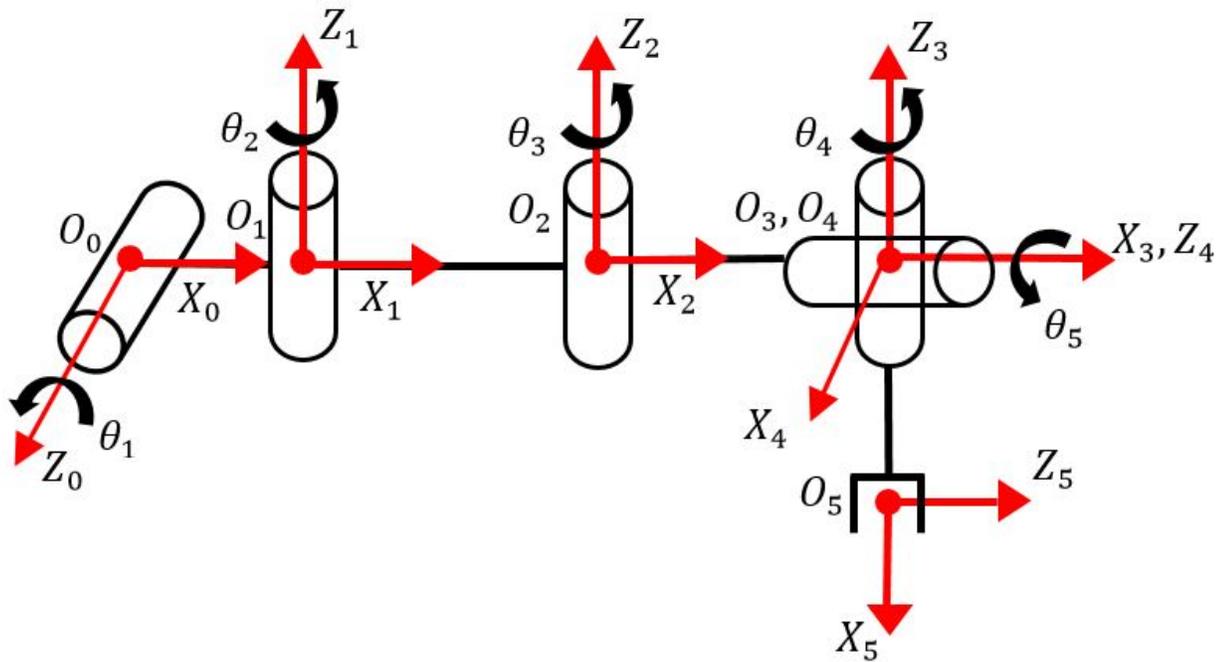
Figure 10 DH frames of exoskeleton
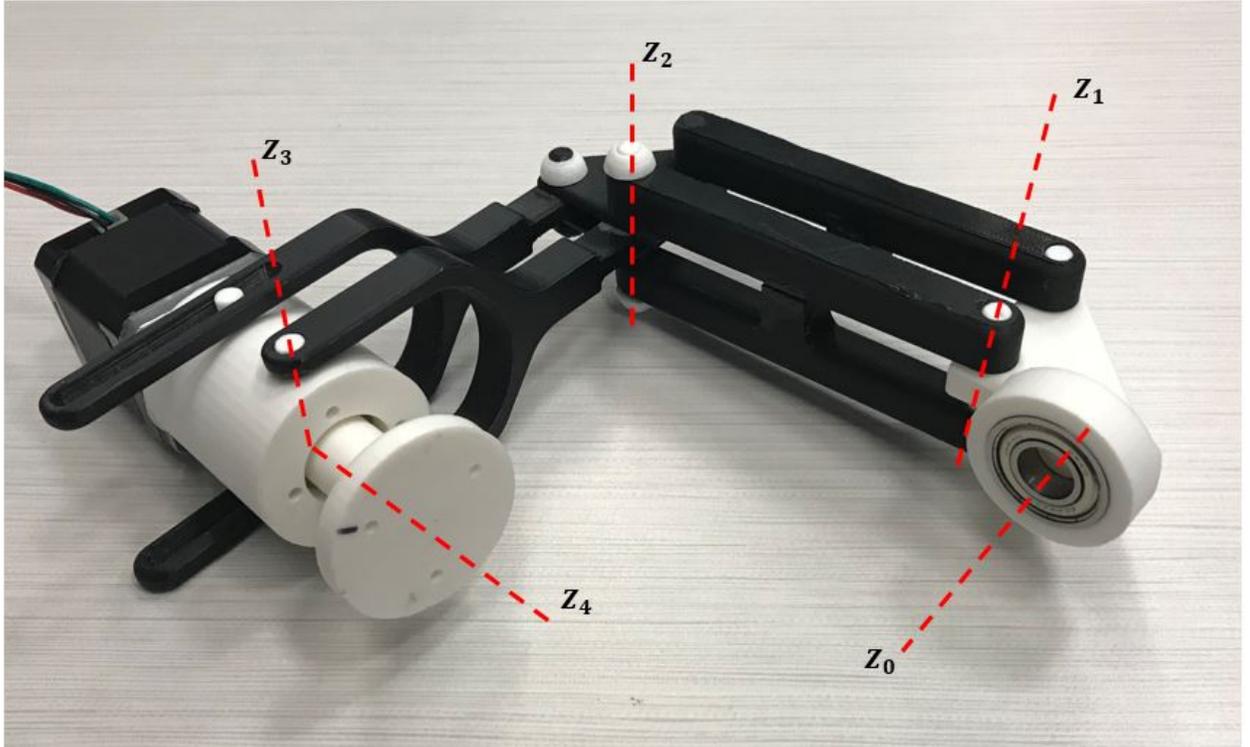
Figure 11 Labeled rotation axes on prototype

A simplified forward kinematic analysis was conducted in which actuation of the exoskeleton was restricted to the transverse plane. Rotation about $\mathbf{z}_0$ is physically responsible for abduction/adduction of the exoskeleton. Rotation θ_4 about $\mathbf{z}_3$ is used to align the mechanism with the upper arm of the wearer and does not affect the range of motion of the exoskeleton. In addition, rotation θ_5 about $\mathbf{z}_4$ corresponds to flexion/extension of the arm of the wearer which does not typically occur in the transverse plane. For the reasons explained above, rotations about $\mathbf{z}_0$, $\mathbf{z}_3$, and $\mathbf{z}_4$ were not included in the forward kinematic analysis. The DH parameters used for the analysis are presented in Table 1.

Table 1. DH parameters for forward kinematic analysis

Link i	a_i (m)	d_i (m)	α_i (°)	θ_i (°)
1	0.0016	0	-90	θ_1^*
2	0.1016	0	0	θ_2^*
3	0.1016	0	0	θ_3^*
4	0	0	90	$\theta_4^* - \dfrac{\pi}{2}$
5	a_5	0	0	$\theta_5^* - \dfrac{\pi}{2}$

The rotation of θ_1 is in the frontal plane and responsible for abduction/adduction. When θ_1 equals 0°, the upper arm of the wearer will be in neutral position. Therefore, when mounted to the wearer, there will be a bracket the exoskeleton can rest on that will prevent θ_1 rotation below 0°. This configuration was assumed for the forward kinematic analysis. The rotation of θ_2 is independent of every other rotation in the mechanism and has a range of -61° to +58°. While θ_3 can rotate independently of θ_2, the range that θ_3 can rotate within is dependent upon the angle of θ_2. For instance, when θ_2 equals -61°, θ_3 has a rotation range from 83° – 152°. However, when θ_2 equals 58°, θ_3 has a rotation range from -30° – 97°. As θ_2 increases, the bounds of θ_3 rotation decreases while its rotation range increases. The rotation of θ_4 solely aligns the end effector with the upper arm of the wearer and has no bearing on forward kinematics. The rotation of θ_5 actuates flexion/extension, and therefore, is only limited by the anatomical range of motion of the wearer. Since the exoskeleton was not in zero angle position when the DH parameters

were determined, both θ_4 and θ_5 require an offset of -90° to accurate record the rotation angles. The kinematic analysis conducted does not include the rotation of either θ_4 or θ_5.

To conduct the forward kinematic analysis a MATLAB program was created to plot the position of $O_3 = O_4$ as θ_2 and θ_3 rotated through their ROMs. For the first value of θ_2, -61°, the entire range of θ_3 was tested. After the rotation of θ_3 was exhausted, the value of θ_2 was increased by 1°, and the range of θ_3 was tested again. These steps were repeated for the entire range of θ_2 angles. This process ensured all angles of θ_2 and θ_3 rotation were examined and recorded. The point of interest, $O_3 = O_4$, is a negligible distance from where the mechanism will attach to the upper arm of the wearer, and accurately represents the range of motion of the exoskeleton. Again, the analysis was conducted for a test case where the exoskeleton begins in a configuration corresponding to the upper arm in neutral position and actuates through its ROM in the transverse plane. The rotation matrices of links 2 and 3 were calculated using Equation 1 below.

Equation 1

$$^{i-1}\mathbf{R}_i = \mathbf{R}_{Z_{i-1}}(\theta_i) * \mathbf{R}_{X_i}(\alpha_i)$$

The rotation matrices were used to determine the position vector for each link using Equation 2.

Equation 2

$$^{i-1}\mathbf{d}_{i-1,i} = d_i * {}^{i-1}\mathbf{z}_i + a_i * {}^{i-1}\mathbf{R}_i * {}^{i-1}\mathbf{x}_i$$

Finally, the position vector for links 2 and 3 were added together to yield the vector connecting O_1 to $O_3 = O_4$ using Equation 3.

Equation 3

$$^1\mathbf{d}_{1,3} = {}^1\mathbf{d}_{1,2} + {}^1\mathbf{R}_2 * {}^2\mathbf{d}_{2,3}$$

Repeating this process for every θ_2 and θ_3, will yield a plot that depicts the locations the exoskeleton can reach in the transverse plane. A resolution of 1° was utilized during plotting.

The results of the forward kinematic analysis are presented in Figure 12 below. Figure 12 is the map of where $O_3 = O_4$ can be positioned relative to O_1 in the transverse plane. The orientation of the end effector is handled by the sliding-pin joint of link (2) and (6). This joint allows the end effector to remain perpendicular to the arm of the wearer during any actuation of the mechanism.
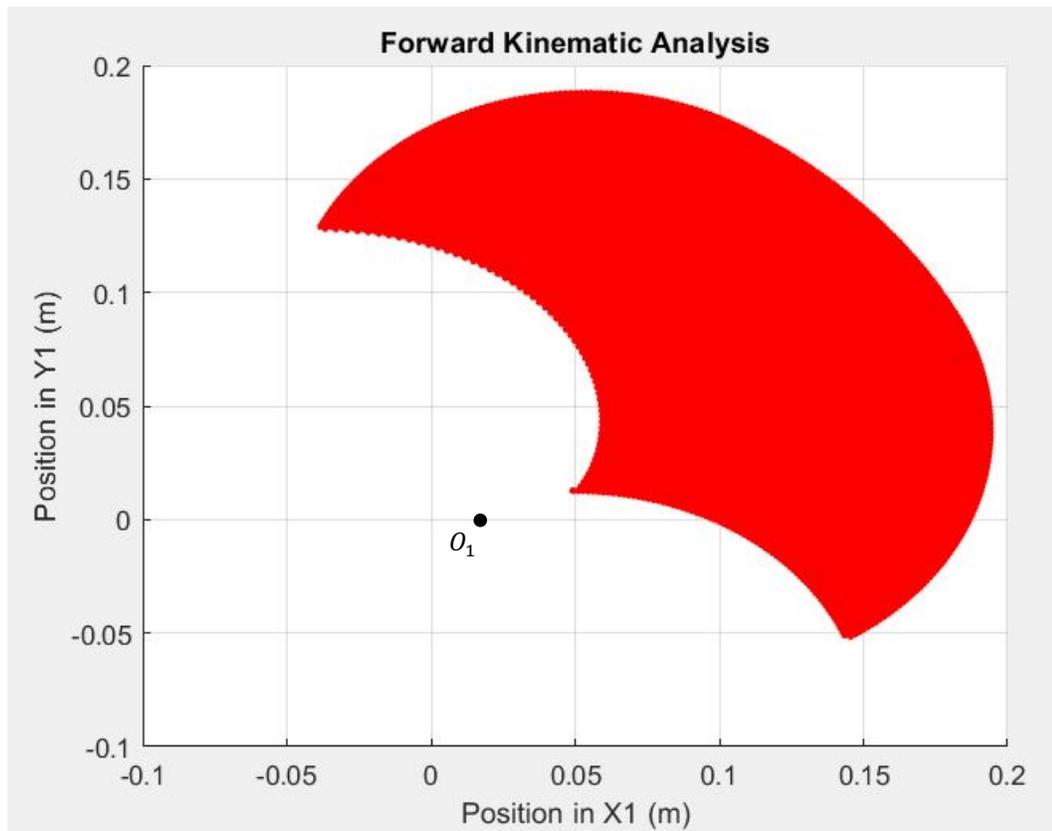
Figure 12 Forward kinematic analysis results of modified DPM shown in the transverse plane formed by x_1 and y_1

To clarify the range of motion achievable by the mechanism Figure 1313**Error! Reference source not found.** is presented below. Figure 1313-A demonstrates an example of the exoskeleton placement on a wearer, and Figure 1313-B demonstrates the

27

achievable ROM. The exoskeleton will be mounted to the wearer with the frame of an Alice Backpack. It is worth noting O_1 is located at (0,0), and is close to where the exoskeleton will be mounted onto wearers.
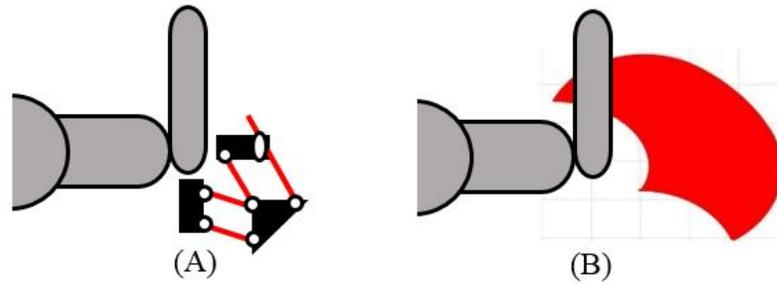
Figure 13 Example modified DPM configuration with ROM

A second analysis was conducted which examined the flexion/extension arm swing achievable by the exoskeleton; this corresponds to θ_5 rotation. In reality, θ_5 can achieve an infinite number of rotations in either direction, clockwise or counterclockwise. In other words, there is not a mechanical limitation that prevents rotation about Z_4. Instead, the mobility of the wearer will determine the rotation limitation of θ_5. A simplified analysis plotted the achievable arm swing trajectory assuming the following configuration parameters. The same MATLAB program discussed previously was utilized when conducting this analysis.

Table 2 Flexion/Extension analysis parameters

Parameter	Value
a_5	0.1778 m
θ_1	0°
θ_2	0°

θ_3	90°
θ_5	-120° – 90°

The parameter a_5 is the distance between $\mathbf{z}_4$ and $\mathbf{z}_5$ along $\mathbf{x}_5$. This corresponds to the length of an arm cuff that will attach to the upper arm of the wearer, extending from the humeral head to approximately the middle of the humerus bone. The arm cuff has not been designed yet but has been approximated to 0.1778 meters. The angles of θ_1, θ_2, and θ_3 have been chosen since they place the plane of θ_5 rotation in the sagittal plane. The rotation of θ_4 has been excluded since it only pertains to the orientation of the end effector and does not influence the kinematic analysis. Finally, the rotation of θ_5 has been approximated from the mobility of the author. The results of the flexion/extension kinematic analysis are presented below.
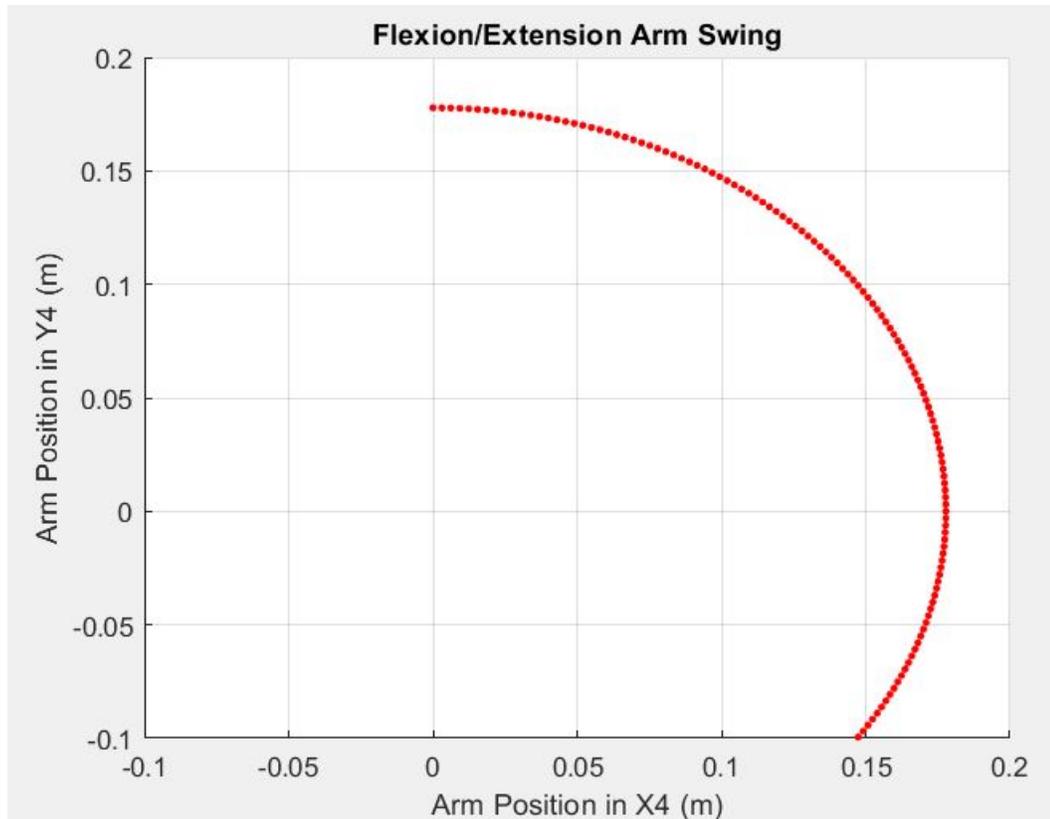
Figure 14 Flexion/Extension kinematic analysis results

PROTOTYPING

A prototype of the exoskeleton was 3D printed out of PLA. The exoskeleton is shown in Figure 15 below. The Figure 15 demonstrates the same configurations as Figure 6—acute, neutral, and obtuse mechanism configurations.

(A)

(B)

(C)
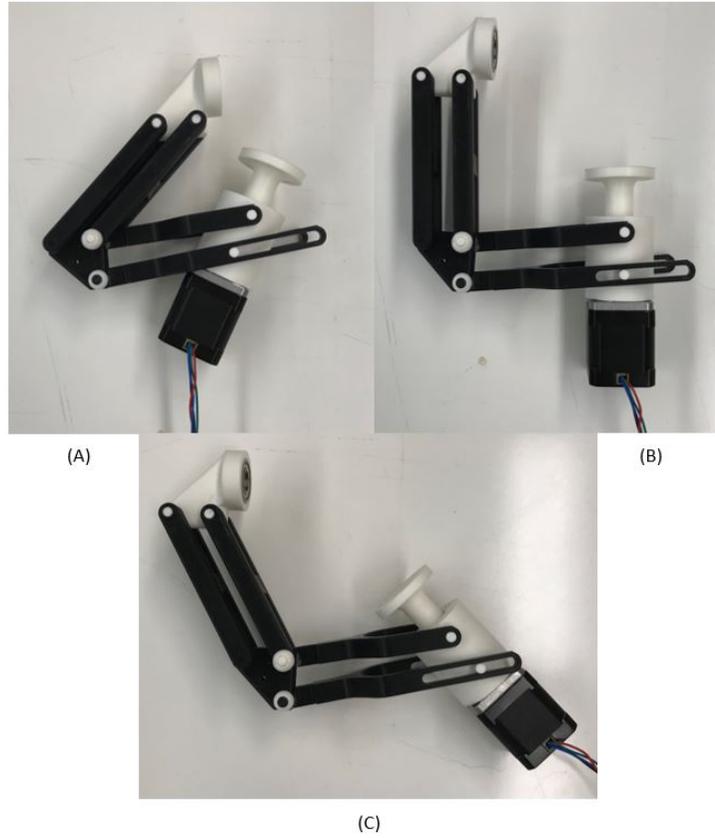
Figure 15 Exoskeleton Configurations, (A) Acute Configuration, (B) Neutral Configuration, (C) Obtuse Configuration

TESTING

To test the exoskeleton a pseudo-shoulder joint was created. The joint was 3D printed out of PLA and includes a cuff that attaches to a foam arm. The arm is only for aesthetic purposes and does not represent the actual weight of a human arm. Figure 16 (A) shows the pseudo-shoulder joint without the exoskeleton mounted, and Figure 16 (B) includes the mounted exoskeleton.

(A)   (B)
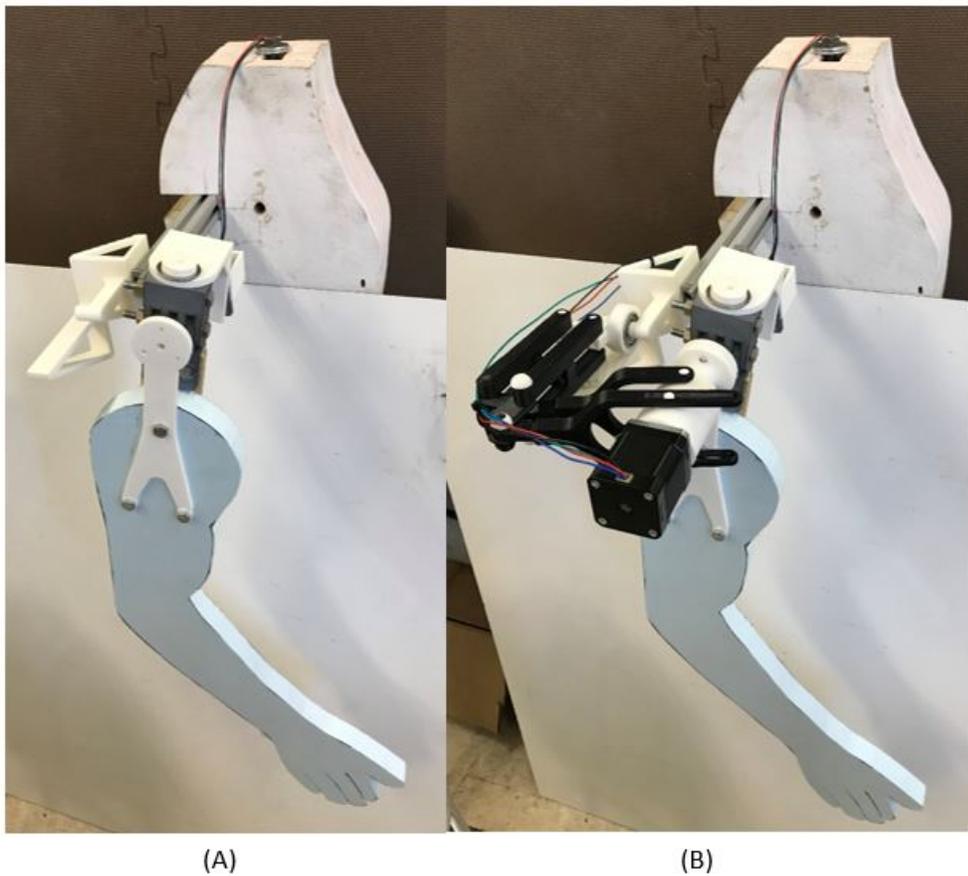
Figure 16 (A) Pseudo-shoulder joint without mounted exoskeleton, (B) Pseudo-shoulder joint with mounted exoskeleton

The shoulder has 3 DOFs, allowing for flexion/extension, abduction/adduction, and internal/external rotation. The size of the joint was determined using approximate shoulder measurements of the author. An axis collinear with the axis of abduction/adduction is used to mount the exoskeleton to the shoulder joint with a rotary bearing. The shoulder joint, with labeled axes, is shown in Figure 177.
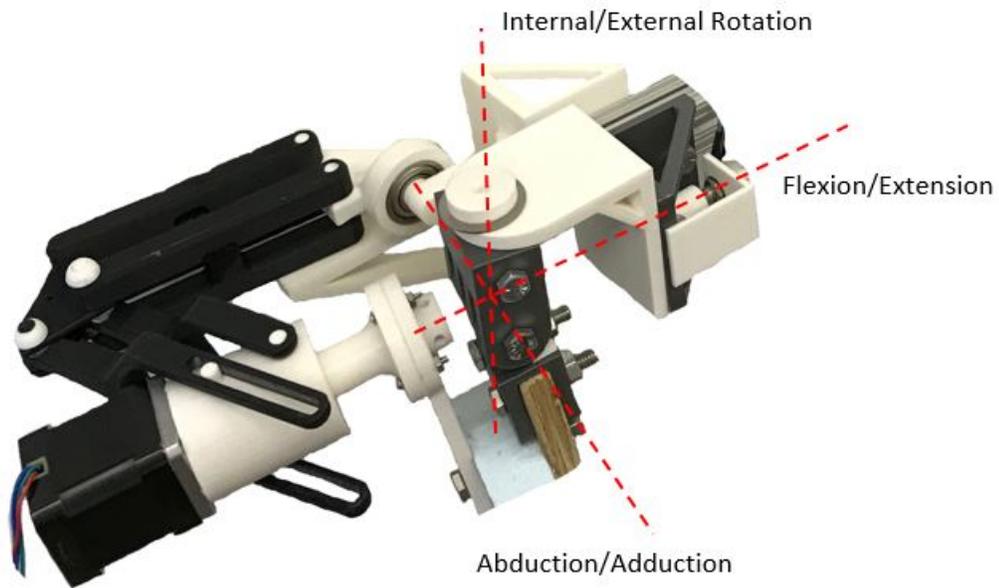
Figure 17 Exoskeleton mounted on pseudo-shoulder

Three tests were conducted to quantify the ROM of the mechanism during flexion/extension. Flexion/extension was tested since it is the movement pattern most used during daily living. Each test varied the angle of internal rotation to ensure flexion/extension can be accomplished at all angles. The three testing orientations are detailed in Table 33 below.

Table 3 Testing scenarios

Test Number	Mechanism Orientation	θ_2 Angle	θ_3 Angle
Test 1	Acute	-2°	45°
Test 2	Neutral	14°	66°
Test 3	Obtuse	47°	100°

It is worth mentioning the orientations of the mechanism described in Table 33 correspond to the orientations depicted in Figure 6 (A), (B), and (C) respectively. In addition, the joint angles tested are all within the boundaries described in Table 1. The acute and obtuse orientation angles were limited by the shoulder stand used for testing. These angles are the maximum angles achievable by the test stand not the mechanism.

To record the rotation of the arm during flexion/extension, a ¾-turn potentiometer was attached to the rotating axis on the shoulder stand. This axis is directly connected to the arm which performs flexion/extension. The potentiometer was supplied with 5V, and the output voltages were read by a Visual Basic program. A Nema 17 stepper motor with a 5.18:1 planetary gearbox was used to actuate the arm. An Arduino Mega and a TB6600 microstep stepper motor driver was used to control the stepper motor. The hardware used is shown below. Based on the motor controller settings and the gearbox ratio, enough pulses were sent to the motor for it to rotate 180 degrees. The Arduino code then switched the direction of rotation for another 180 degrees. This was repeated three times, and was consistent for each test. Presented below are the results for each of the three tests in Table 33.
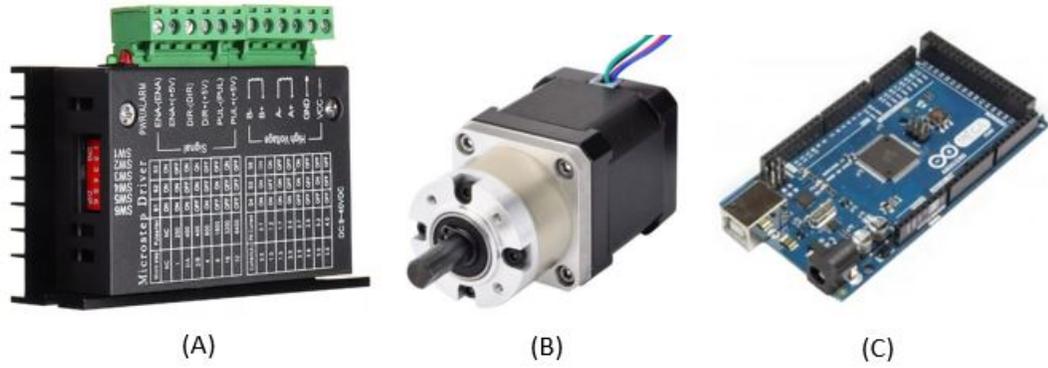
Figure 18. (A) TB6600 microstep stepper motor driver, (B) Nema 17 with 5:1 planetary gearbox, (C) Arduino Mega
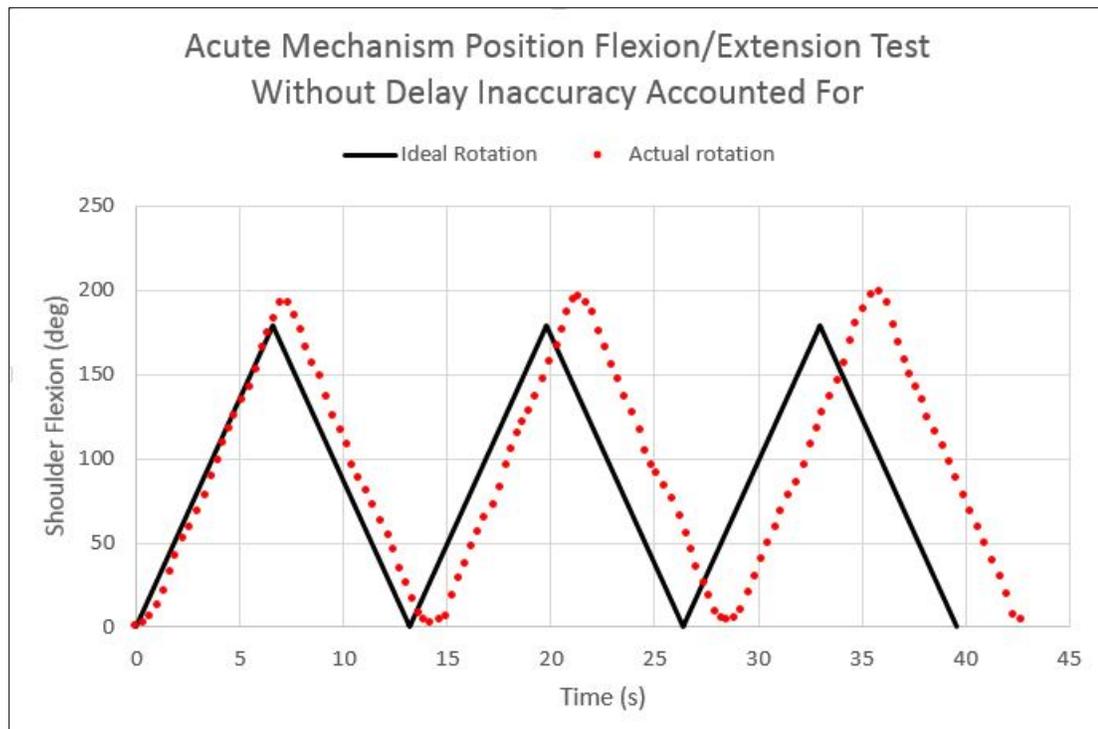
Figure 19 Acute Graph with Offset
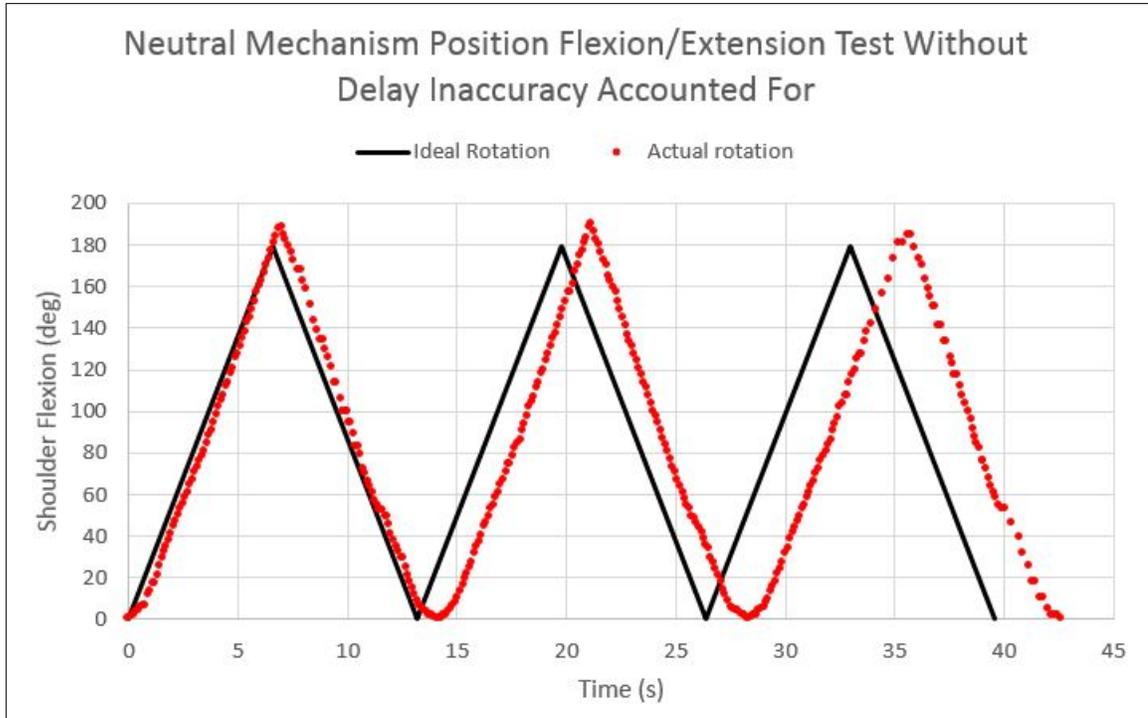
Figure 20 Neutral Graph with Offset
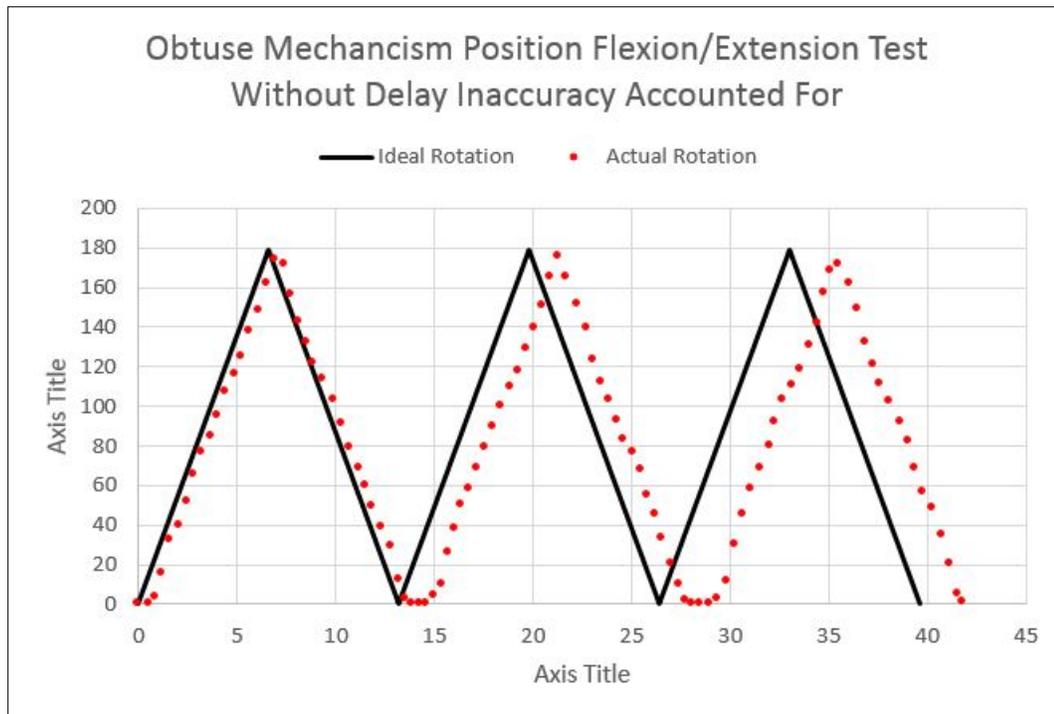
Figure 21 Obtuse Graph with Offset

All of the graphs presented above have a considerable offset from the ideal

rotation. This was found to be due to the '*delay()*' command in Arduino. The logic for

actuating the motor is as follows. The output pin was set to '*HIGH*', this supplies it with

5 volts, and was followed by a 200 microsecond delay using the '*delay ()*' command.

After the delay, the output pin was set to '*LOW*', which supplies 0 volts to the motor, and

was followed by another 200 microsecond delay. This is considered one pulse which

rotates the motor a minuscule amount. A total of 16,576 pulses were required to rotate the

motor the desired 180 degrees. Using an oscilloscope, the actual value of the delay was

determined to be 209 microseconds. Multiplying this inaccuracy by 2, for both the on and

off cycles, and then by 16,576, for each pulse, accounts for the large phase shift seen in

Figure 199, Figure 2020, and Figure 21. Presented below are the modified graphs, whose

ideal rotation lines account for the delay inaccuracy.
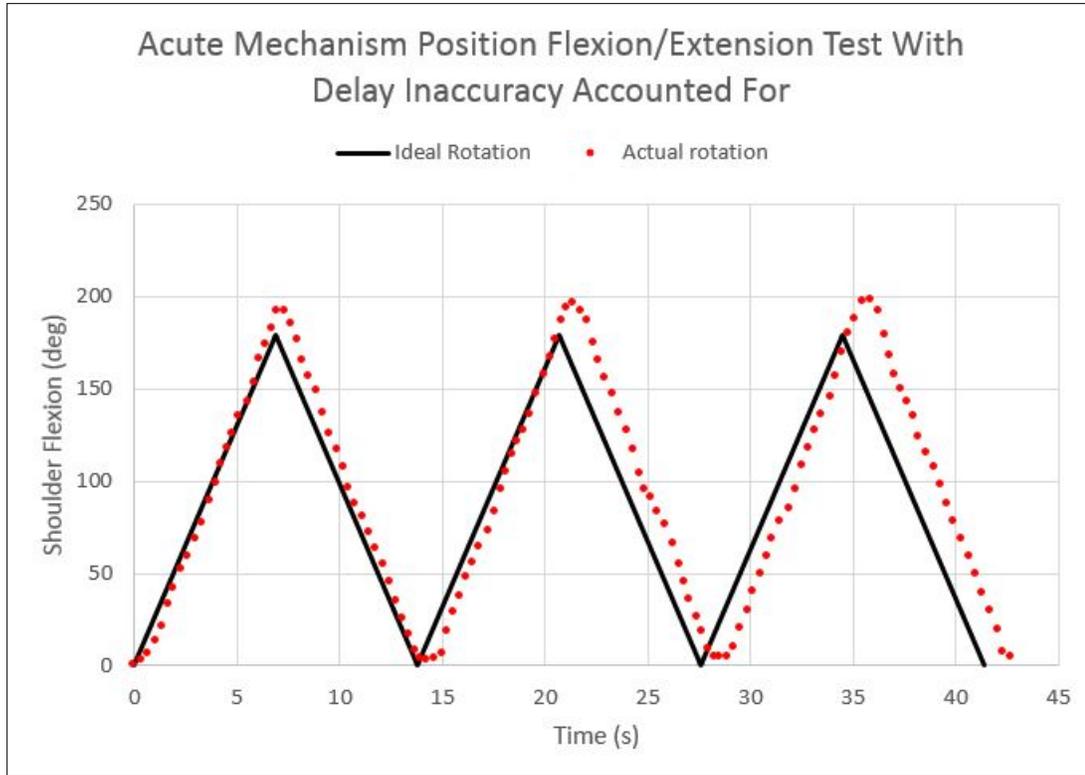
Figure 22 Acute Graph without Offset
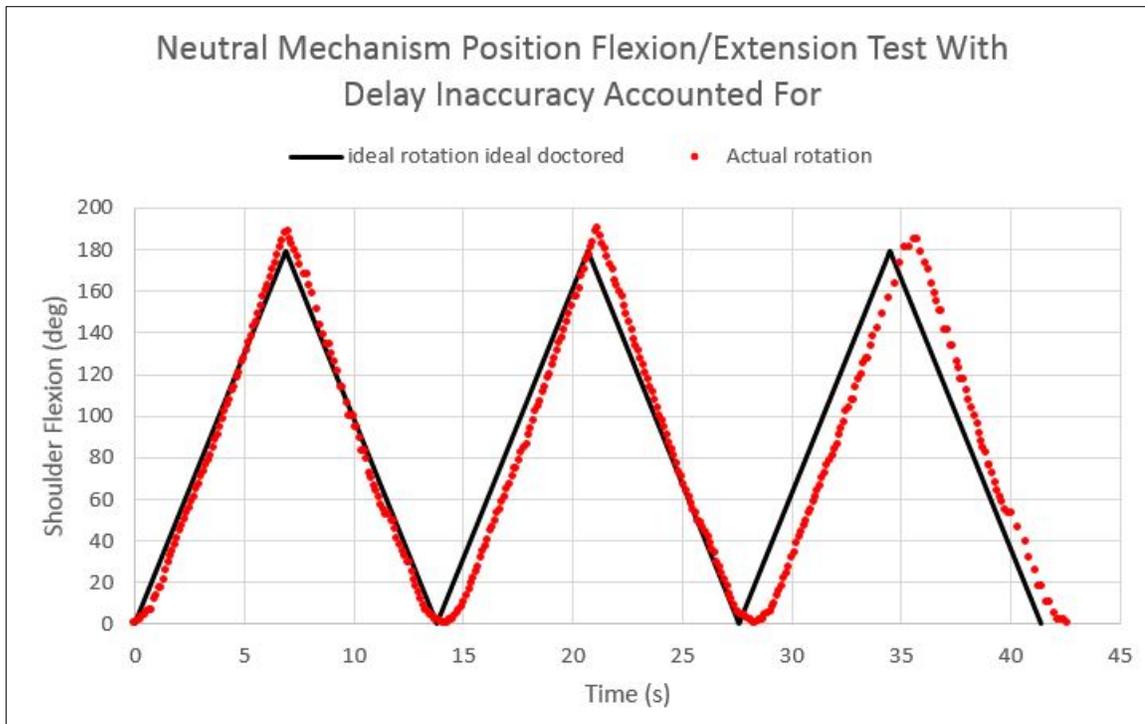
Figure 23 Neutral Graph without Offset

38
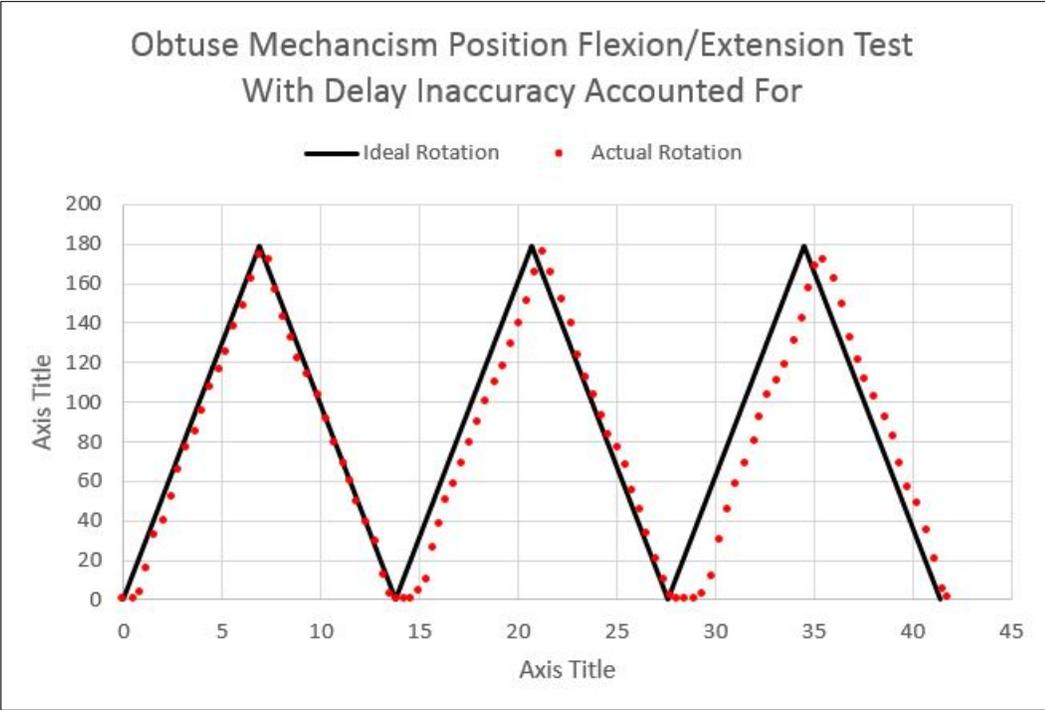
Figure 24 Obtuse Graph without Offset

CONCLUSIONS AND FUTURE WORK

This thesis presents a 3 DOF exoskeleton utilizing a modified DPM. The exoskeleton provides assistance during flexion/extension, with a proximally located actuator, and it is passive during abduction/adduction and internal/external rotation. The modified DPM increases the ROM of the exoskeleton and allows it to fit onto a wide range of anthropomorphic frames. This mitigates the potential for joint misalignment during internal/external rotation. Experiments demonstrated that flexion/extension is possible in acute, neutral, and obtuse mechanism configurations.

Currently, scapular elevation/depression is not a passive DOF allowed by the exoskeleton. Future design iterations will focus on this DOF. In addition, the link lengths and design will be optimized. Finally, the design should be mounted to a backpack so that it can be worn, and an arm cuff must be designed to attach to the arm of the wearer.

REFERENCES

[1]   H. C. Hsieh, D. F. Chen, L. Chien, and C. C. Lan, "Design of a Parallel Actuated Exoskeleton for Adaptive and Safe Robotic Shoulder Rehabilitation," *IEEE/ASME Trans. Mechatronics*, vol. 22, no. 5, pp. 2034–2045, 2017.

[2]   S. Christensen, S. Bai, "Kinematic Analysis and Design of a Novel Shoulder Exoskeleton using a Double Parallelogram Linkage," *J. Mech. Robot.*, vol. 10, no. August, pp. 1–10, 2018.

[3]   L. Peebles and B. Norris, Adultdata: The Handboof of Adult Anthropometric and Strength Measurments. Data for Design Safety, UK: Department of Trade and Industry, 1998.

[4]   K. Kiguchi, "Development of a 3DOF mobile exoskeleton robot for human upper-limb," *Elsevier*, pp. 678-691, 2008.

[5]   R. Vertechy, "Development of a New Exoskeleton for Upper Limb Rehabilitation," *IEEE*, vol. 11, pp. 188-193, 2009.

[6]   H.-S. Park, "IntelliArm: An Exoskeleton for Diagnosis and Treatment of Patients," IEEE, pp. 109-114, 2008.

[7]   J. Pasteris, "How Much Should Your Pack Weigh?," REI Co-op, [Online]. Available: https://www.rei.com/blog/camp/how-much-should-your-pack-weigh. [Accessed 21 December 2018].

[8]   C. Liu, C. Zhu, H. Liang, M. Yoshioka, Y. Murata, and Y. Yu, "Development of a light wearable exoskeleton for upper extremity augmentation," in *2016 23rd International Conference on Mechatronics and Machine Vision in Practice (M2VIP)*, 2016, pp. 1–6.

[9]   H. C. Hsieh, L. Chien, and C. C. Lan, "Mechanical design of a gravity-balancing wearable exoskeleton for the motion enhancement of human upper limb," *Proc. - IEEE Int. Conf. Robot. Autom.*, vol. 2015–June, no. June, pp. 4992–4997, 2015.

[10]   D. Sui, J. Fan, H. Jin, X. Cai, J. Zhao, and Y. Zhu, "Design of a wearable upper-limb exoskeleton for activities assistance of daily living," in *2017 IEEE International Conference on Advanced Intelligent Mechatronics (AIM)*, 2017, pp. 845–850.

[11]   C. Carignan, M. Liszka, and S. Roderick, "Design of an arm exoskeleton with scapula motion for shoulder rehabilitation," *2005 Int. Conf. Adv. Robot. ICAR '05, Proc.*, vol. 2005, pp. 524–531, 2005.

[12] A. Ebrahimi, "Stuttgart Exo-Jacket: An exoskeleton for industrial upper body applications," in *2017 10th International Conference on Human System Interactions (HSI)*, 2017, pp. 258–263.

[13] N. Vitiello, "NEUROExos: A Powered Elbox Exoskeleton for Physical Rehabilitation," *IEEE,* vol. 29, no. 1, pp. 220-235, 2013.

[14] K.Y. Wu, "Series Elastic Actuation of an Elbow Rehabilitation Exoskeleton," *IEEE*, pp. 567-572, 2017.

[15] L. Cappello, D. K. Binh, S. C. Yen, and L. Masia, "Design and preliminary characterization of a soft wearable exoskeleton for upper limb," *Proc. IEEE RAS EMBS Int. Conf. Biomed. Robot. Biomechatronics*, vol. 2016–July, pp. 623–630, 2016.

[16] B. K. Dinh, "Adapative backlash compensation in upper limb soft wearable exoskeletons," *Elsevier,* pp. 173-186, 2017.

[17] D. Abe, S. Muraki, and A. Yasukouchi, "Ergonomic effects of load carriage on the upper and lower back on metabolic energy cost of walking," vol. 39, pp. 392–398, 2008.

[18] K. M. Simpson, B. J. Munro, and J. R. Steele, "Does load position affect gait and subjective responses of females during load carriage ?," *Appl. Ergon.*, vol. 43, no. 3, pp. 479–485, 2012.

AUTHOR'S BIOGRAPHY

Connor Bouffard was born in Honolulu, Hawaii on December 31st 1996. After only 9 months of life on the island, he was packed up and moved to Greenwood, Indiana. There he stayed for approximately 7 years, doing things most Hoosiers do—filling his belly with biscuits and gravy. At the age of 8, however, him and his family packed up and moved to southern Maine where he would live out the majority of his adolescent life. In high school, he participated in many clubs and sports teams, and could be appropriately described as a studious, social butterfly. The state of Maine seemed to resonate with young Bouffard, and he decided to further his education at the University of Maine at Orono. During the summers of his college career he spent time working at multiple internships which eventually lead to a job offer at Texas Instruments. On July 15th 2019, he will officially become a Manufacturing Engineer at T.I. and the next chapter of his life will begin. Thank you for participating in the thesis process.